nutraceuticals

MDPI

Article

DPP-IV Inhibition by Solubilized Elastin Peptides from Yellowtail Bulbus Arteriosus Suppresses Ultraviolet-B-Induced Photoaging in Hairless Mice

Kumiko Takemori [1,2,3,*,†], Ei Yamamoto [4,†], Takaaki Chikugo [5], Eri Shiratsuchi [6] and Takashi Kometani [1,7]

[1] Department of Food and Nutrition, Faculty of Agriculture, Kindai University, 3327-204 Nakamachi, Nara 631-8505, Japan
[2] Agricultural Technology and Innovation Research Institute, Kindai University, 3327-204 Nakamachi, Nara 631-8505, Japan
[3] Antiaging Center, Kindai University, 3-4-1 Kowakae, Higashiosaka 577-8502, Japan
[4] Department of Medical Engineering, Faculty of Biology-Oriented Science and Technology, Kindai University, 930 Nishimitani, Kinokawa 649-6493, Japan; ei@waka.kindai.ac.jp
[5] Department of Pathology, Faculty of Medicine, Kindai University, 377-2, Ohno-Higashi, Osaka-Sayama 589-8511, Japan
[6] R & D Division, Hayashikane Sangyo Co., Ltd., 2-4-8 Yamato-machi, Shimonoseki 750-8608, Japan
[7] Pharma Foods International, Co., Ltd., 1-49 Goryo-Ohara, Nishikyo-ku, Kyoto 615-8245, Japan
* Correspondence: kuriman@nara.kindai.ac.jp
† These authors contributed equally to this work.

Abstract: Skin aging is intrinsic and extrinsic. Intrinsic, or chronological, skin aging is an inevitable process of chronological and physiological alterations. The factors contributing to extrinsic skin aging involve sunlight, nutrients, and stress. Thus, extrinsic aging is thought to be superimposed over intrinsic aging and depends on the intensity and duration of environmental exposure and skin type (e.g., dry skin, oily skin, or eczema). The most significant extrinsic aging factor is UV radiation, which causes cellular senescence in a process known as photoaging. This study aimed to illuminate the mechanism whereby solubilized elastin peptide lotion (EL) from the bulbus arteriosus of yellowtail (*Seriola quinqueradiata*) prevents skin photoaging in hairless mice. EL reduced wrinkle formation, epidermal skin thickness, and *Ki67* (cell growth marker) mRNA expression in skin tissues from ultraviolet B (UVB)-irradiated mice. EL treatment also reduced glyoxalase-1 (key enzyme of glucose metabolism) levels in skin tissue. Although no significant differences in collagen and elastin contents were found in dermal areas, matrix metalloproteinase-12 (wrinkle-related marker) expression was reduced following EL application. Furthermore, skin DPP-IV/CD26 (new senescence marker) levels decreased following EL treatment in photoaging model mice. These results suggest that EL moderates skin damage caused by UVB irradiation by regulating senescence-related molecule expression.

Keywords: elastin peptide; DPP-IV/CD26 inhibition; photoaging

Citation: Takemori, K.; Yamamoto, E.; Chikugo, T.; Shiratsuchi, E.; Kometani, T. DPP-IV Inhibition by Solubilized Elastin Peptides from Yellowtail Bulbus Arteriosus Suppresses Ultraviolet-B-Induced Photoaging in Hairless Mice. *Nutraceuticals* **2024**, *4*, 683–694. https://doi.org/10.3390/nutraceuticals4040038

Academic Editor: Ronan Lordan

Received: 20 October 2024
Revised: 2 December 2024
Accepted: 3 December 2024
Published: 5 December 2024

1. Introduction

The skin is an organ that protects the body against moisture loss and forms a barrier against extrinsic harmful substances and physical damage under normal conditions. Alterations in skin structure, function, and appearance are more pronounced in external photoaged skin than internal chronologically aged skin [1–3]. However, these two types of aging are difficult to separate and are superimposed in sun-exposed skin, as they have common features caused by dermal matrix alterations that contribute to wrinkle formation and laxity. The dermal matrix contains extracellular matrix (ECM) proteins such as collagen and elastin, which confer skin strength and resilience [2]. Skin aging associated with dermal matrix alterations can be caused by the senescence of dermal cells such as fibroblasts, and decreased synthesis and accelerated breakdown of dermal collagen and elastic fibers [3].

Skin photoaging involves histological and functional changes in chronically sun-exposed skin. Ultraviolet radiation (UV) is divided into three types according to wavelength: UVA (UVA) (315–400 nm); UVB (280–315 nm); and UVC (100–280 nm) [1]. Long-term overexposure to UVB usually induces photoaging and damages the skin epidermis and dermis [2]. Continuous UVB exposure induces wrinkle formation and increases epidermal skin thickness and laxity [3]. UVB causes DNA damage and generates reactive oxygen species (ROS) in the skin, eventually leading to skin aging [1,4]. UVB is also closely correlated with advanced glycation end products (AGEs) accumulation in the skin [5]; UV-induced ROS accelerate AGEs formation, which plays a crucial role in the AGEs-related modification of elastic fibers, resulting in solar elastosis [6].

These changes are closely associated with matrix metalloproteinases (MMPs), which are zinc-containing endopeptidases that degrade various constituents of the ECM such as collagen and elastin. They can be categorized into six main groups: (1) collagenases (MMP-1, 8, and 13); (2) gelatinases (MMP-2 and 9); (3) stromelysins (MMP-3, 10, and 11); (4) matrilysins (MMP-7 and 26); (5) metroelastase (MMP-12); and (6) membrane-type MMPs (MMP-14, 15, MMP-16). The alterations to the ECM induced by MMPs might contribute to skin wrinkling, a characteristic of premature skin aging. In chronological aging and photoaging, degradation of the ECM is the initial step [3]. ECM proteins are involved in the matrix barrier, balance, and extrinsic factor protection functions of skin. However, UV induces the upregulated expression of MMPs in keratinocytes and dermal fibroblasts, eventually leading to photoaging, inflammation, and skin cancer [7]. Therefore, these markers must be regulated to protect the skin against UV-induced photoaging and have been the focus of ongoing research.

Recently, dipeptidyl peptidase IV (DPP-IV)/CD26 has attracted increasing attention. The most important catalytic function is the inactivation of incretin hormones (e.g., glucose-dependent insulinotropic polypeptide hormone (GIP) and glucagon-like peptide 1 (GLP-1)). DPP-IV inhibitor is a hypoglycemic agent that regulates incretin activity, and subsequently decreases blood glucose levels [8]. Studies on DPP-IV/CD26 have yielded some promising results regarding senescence [9,10]. DPP-IV/CD26 has been shown to regulate T cells, macrophages, fibroblasts, keratinocytes, adipocytes, and endothelial cells, which are the major cells involved in wound healing and scar formation [11], in various ways, implying that DPP-IV/CD26 might play an important role in the processes of wound healing and scar formation. However, the beneficial effects of DPP-IV/CD26 inhibition on photoaging remain unclear. Some synthetic DPP-IV/CD26 inhibitors are currently available, but they entail a risk of side-effects, including gastrointestinal and skin reactions [12]. Thus, some natural functional components, such as proteins and peptides, have been screened for inhibitory activity against DPP-IV/CD26 [13,14], and these peptides are receiving increasing attention due to their high potency, selectivity, and safety.

Elastic fibers are essential constituents of the ECM and underlie the elasticity and resilience of tissues and organs, including the lungs, skin, and blood vessels. During the aging process, elastic fibers are exposed to a variety of enzymatic, chemical, and biophysical influences and accumulate damage due to their low turnover [15]. We have previously reported that prolylglycine, a fish-derived elastin peptide, has a protective effect on vascular endothelial cells [16]. However, whether this peptide displays anti-photoaging activity remains unknown. In this study, we further studied the DPP-IV/CD26 inhibitory activity of elastin peptides derived from the bulbus arteriosus of yellowtail (*Seriola quinqueradiata*) and examined their effects on skin damage in photoaging model mice.

2. Materials and Methods

2.1. Sample Preparation

Yellowtail bulbus arteriosus provided by Hayashikane Sangyo Co., Ltd. (Shimonoseki, Yamaguchi, Japan) were used as the experimental materials. After the adipose tissue and capsule around the yellowtail bulbus arteriosus were removed, elastin was purified and solubilized according to the method of Halabi et al., with slight modification [17].

Briefly, the bulbus arteriosus was washed with 1% NaCl solution and homogenized using a Polytron homogenizer (PT-MR2100, Kinematica, Malters, Canton of Lucerne, Switzerland) and a Potter homogenizer (SER. No 721 03048, Panasonic Co., Osaka, Japan). The sample was centrifuged (2280× *g*, 10 min, 4 °C, MX-307, Tomy Seiko Co., Ltd., Tokyo, Japan), and the supernatant was discarded three times to remove salt-soluble proteins. Washed tissue was autoclaved in 20 volumes of distilled water at 120 °C for 45 min (HG-50, Hirayama Manufacturing Co., Kasukabe, Saitama, Japan), and a 30% trichloroacetic acid solution was added to the supernatant to remove proteins. The autoclaving step was repeated with fresh distilled water until no further protein was detected in the supernatant. The residue was defatted and dehydrated using the following series of solutions: 100% ethanol (10 min, three times), a 1:1 (*v*/*v*) ethanol/ether mixture (15 min, two times), and 100% ether (10 min, three times). Thereafter, the precipitate was vacuum dried overnight using a vacuum pump (GLD-051, ULVAC Kikai Co., Ltd., Saito, Miyazaki, Japan) to obtain insoluble elastin. Purified elastin was then obtained using the hot alkali method of Lansing et al. [18]. Furthermore, to obtain solubilized elastin peptide, purified elastin was hydrolyzed with 0.25 M oxalic acid at 100 °C for 1 h according to the method of Partridge et al. [19,20]. To obtain solubilized elastin peptide, purified elastin was hydrolyzed with oxalic acid according to the method of Partridge et al. Oxalic acid in the treated solution was removed by dialysis (Spectra/Por Dialysis Membrane MWCO: 6000–8000, Spectrum Laboratories Inc., Compton, CA, USA) until a pH of 4–6 was reached.

When the final yellow solution (dialysate) was warmed to 37 °C at pH 4–6, a "coacervate", consisting of a self-associated elastin fraction (α-elastin), was formed, and then the coacervate (the lower layer) was separated from the clear solution (β-elastin) by centrifugation. The purified α- and β-elastin solutions were freeze dried (FDM-1000, Tokyo Rikakikai Co., Ltd., Tokyo, Japan) to obtain powdered materials. The α- and β-elastin fractions contain peptides with molecular weights of 60,000 to 84,000 and less than 5000, respectively [17]. The β-elastin powder was used in this experiment.

2.2. Amino Acid Composition of Elastin Peptides

α- and β-elastin were dissolved in lithium citrate buffer (JEOL Ltd., Tokyo, Japan). The composition and content of amino acids in the elastin peptides were determined with an automatic analyzer according to the methods of Nakaba et al. [21].

2.3. SDS-PAGE

To confirm the molecular weight distribution of α- and β-elastin, sodium dodecyl sulfate–polyacrylamide gel electrophoresis (SDS-PAGE) was carried out. The sample solution and 2 × sample buffer (with or without 10% 2-mercaptoethanol) were mixed at a ratio of 1:1 and then boiled for 5 min. Then, 20 μg of each sample was added to separate lanes of a 5–20% polyacrylamide gradient gel. SDS-PAGE (90 min, 20 mA/gel) and silver staining (Silver stain II Kit Wako, Fujifilm Wako Pure Chemicals. Co., Osaka, Japan) were carried out according to the manufacturer's instructions.

2.4. DPP-IV Inhibition Assay

The sample employed for this assay consisted of 1% β-elastin/0.2 M Tris-HCl buffer (pH 7.0). DPP-IV inhibitory activity was performed using the DPP(IV) Inhibitor Screening Assay Kit (Cayman Chemical, Ann Arbor, MI, USA) according to the manufacturer's instructions. The fluorescence intensity was measured at an excitation wavelength of 355 nm and an emission wavelength of 460 nm (ARVOTM MX 1420 Multilabel Counter, 46205628, PerkinElmer Inc., Waltham, MA, USA). The percent inhibition was expressed as the ratio to Sitagliptin, the positive control inhibitor.

2.5. Animals and Experimental Groups

Male hairless mice (Hos:HR-1, 18 weeks old) were used in this study (Japan SLC, Inc. Hamamatsu, Shizuoka, Japan). The animals were kept at a temperature of

23 ± 1 °C and humidity of 55 ± 5% under a 12 h light/dark cycle, housed in standard cages (3 mice per cage), and given free access to a standard laboratory diet (Labo MR Stock, Nosan Co., Yokohama, Kanagawa, Japan) and water. Prior to the experiment, all animals were acclimatized for 7 days. The experimental protocol was approved by Kindai University Animal Experiment Committee and was conducted while strictly adhering to the Kindai University Animal Experiment Regulations (approval number: KAAG-25-010).

For the experiment, 24 mice were randomly divided into four groups (6 mice in each group) as follows: (1) Control: mice not exposed to UVB; (2) UV: UVB exposure; (3) PL: mice where placebo lotion was applied to the dorsal skin after UVB exposure; (4) EL: mice where 1% β-elastin lotion was applied to the dorsal skin after UVB exposure. Lotion containing absolute ethanol and polyethylene glycol at a ratio of 7:3 (v/v) was used. Placebo lotion and 1% β-elastin lotion were applied immediately after each UVB exposure.

2.6. Preparation of the Photoaged Mouse Model

Preparation of the photoaged mouse model was established according to the methods of Kawada et al. [22], with slight modification. The irradiation intensity was set at 1.5 mW/cm^2 by adjusting the distance between the handheld UV lamp (302 nm, Model UVP UVM-57, Analytik Jena, Thuringia, Germany) and the animal. To deliver a total irradiation dose of 2286 mJ/cm^2, irradiation was continued once every two days for 18 weeks, and the irradiation time and dose were increased each week. Mice were exposed to UVB radiation two times a week, starting with 36 mJ/cm^2 for 24 s (first week), followed by 54 mJ/cm^2 for 36 s (second week), then 72 mJ/cm^2 for 48 s (third week), and 108 mJ/cm^2 for 72 s (fourth week). Exposure was maintained at 144 mJ/cm^2 for 96 s for the remaining weeks.

The dorsal skin of the mice was photographed under anesthesia performed using a combination of pentobarbital sodium salt (Nacalai Tesque Inc., Kyoto, Japan) and isoflurane (Fujifilm Wako Pure Chemical Co., Osaka, Japan) at the end of the study. All dorsal skin samples were divided into two parts. One part was quickly cut, precisely weighed, fixed with 10% formalin neutral buffer solution for at least 24 h, dehydrated with an ethanol concentration gradient series, and embedded in paraffin for future histopathologic observations. The second part was soaked with RNA Later solution (Thermo Fisher Scientific Inc., Waltham, MA, USA) overnight and kept at −80 °C prior to Real-Time polymerase chain reaction (RT-PCR) analysis.

2.7. Histological Examination

Paraffin-embedded dorsal skin tissues were placed on glass slides, cut into thin slices (2.5 μm) with a sliding microtome (Sakura Finetek Japan Co., Ltd., Tokyo, Japan), deparaffinized with xylene, and rehydrated in a graded alcohol series. Structural changes in the skin were assessed microscopically via hematoxylin–eosin (HE) and **Elastica Van Gieson (EVG) staining**. To evaluate epidermal thickness following UVB exposure, 30 areas of the epidermis per slide in randomly selected locations were measured using the BZ-H3 application on an All-in-One Fluorescence Microscope BZ-X800E (Keyence, Osaka, Japan).

2.8. Real-Time Polymerase Chain Reaction (RT-PCR)

Total RNA was extracted from the remaining part of the skin using the RNeasy Tissue and RNeasy Fibrous Tissue Mini-kit (Qiagen, Valencia, CA, USA). The optical density of the samples was measured at 230, 260, and 280 nm on an e-Spect ES2 Spectrophotometer (BM Equipment Co., Ltd., Tokyo, Japan). Total RNA was reverse transcribed using an ExScript RT Reagent kit (Applied Biosystems, Carlsbad, CA, USA). RT-PCR was carried out using an ABI PRISM® 7900HT system (Applied Biosystems) with SYBR Premix Ex Taq II (Tli RNaseH Plus) (Takara Bio Inc., Shiga, Japan). Specific primers were purchased from Takara Bio Inc. Each mRNA expression was evaluated as the ratio relative to GAPDH.

2.9. Statistical Analysis

Results are expressed as the mean ± standard deviation of the mean (SD). SPSS 29 Statistics Base AC (IBM, Armonk, NY, USA) was used for statistical analysis. Tukey's honestly significant difference test or Dunnett's test was used, depending on the results of the Shapiro–Wilk normality test and ANOVA. A p-value of <0.05 was considered statistically significant.

3. Results

3.1. Amino Acid Composition of Elastin Peptides from Yellowtail Bulbus Arteriosus

Table 1 shows the amino acid composition of α-elastin and β-elastin obtained from the yellowtail bulbus arteriosus. Desmosine (Des) and isodesmosine (Ide) are crosslinking amino acids of elastin, which is an essential protein component of the ECM. It was confirmed that both α-elastin and β-elastin contained desmosine and isodesmosine. In addition, the amino acid composition was consistent with a previous report [21].

Table 1. Amino acid composition of elastin peptides from yellowtail bulbus arteriosus.

	α-Elastin	**ß-Elastin**
Asp	23.030 [1]	41.939
Thr	55.268	57.768
Ser	37.580	44.816
Glu	49.625	75.623
Gly	388.831	320.536
Ala	110.174	103.193
Val	55.121	58.025
Cys	1.116	1.082
Met	6.669	11.275
Ile	14.881	21.859
Leu	48.736	55.661
Thr	46.262	37.254
Phe	23.334	24.787
His	3.808	6.385
Lys	11.476	21.047
Arg	23.051	25.869
Hyp	6.102	5.230
Rro	93.216	86.391
Ide	0.830	0.615
Des	0.892	0.645
Total	1000	1000

[1] Results are expressed as amino acid residues/1000 total residues.

3.2. Molecular Weight Distribution of Elastin Peptides from Yellowtail Bulbus Arteriosus

SDS-PAGE was performed on each sample of solubilized elastin under reducing and non-reducing conditions. A prestained EX ladder (Apro Science Group/Pharma Foods International Co., Ltd., Tokushima, Japan) was used as a molecular weight marker. α-Elastin from the yellowtail bulbus arteriosus showed a broad molecular weight distribution, mainly concentrated around 20 to 150 kDa. The distribution of β-elastin was mainly in the low-molecular-weight region below 35 kDa (Figure 1).

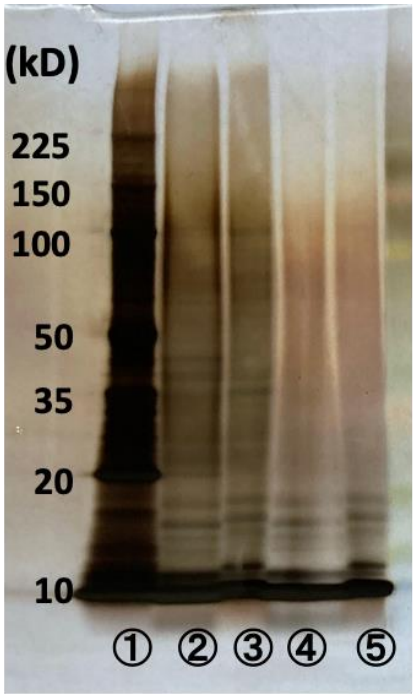

Figure 1. Electrophoretic pattern of α- and β-elastin. ① Molecular weight marker; ② α-elastin with 10% 2-mercaptoethanol; ③ α-elastin without 10% 2-mercaptoethanol; ④ β-elastin with 10% 2-mercaptoethanol; ⑤ β-elastin without 10% 2-mercaptoethanol.

3.3. DPP-IV Inhibition Activity of Elastin from Yellowtail Bulbus Arteriosus

DPP-IV inhibition by each form of solubilized elastin was investigated. Yellowtail-derived α-elastin was inhibited by 52.5% and β-elastin by 57.5%.

In subsequent experiments, β-elastin, which exhibits a low-molecular-weight distribution and a high yield after oxalic acid decomposition, was used (0.04% yield of α-elastin, 3.4% yield of β-elastin from the yellowtail bulbus arteriosus).

3.4. Macroscopic Findings in the Dorsal Skin of Hairless Mice

Figure 2 shows the macroscopic findings for the dorsal skin of hairless mice. Roughness, wrinkle formation, thickening, and hardening of the skin surface were observed in the UV group (B) compared with the Control group (A), which was not treated with UVB irradiation. However, the surface skin of the PL (C) and EL (D) mice remained smooth and flexible.

3.5. Histological Findings

To estimate the effects of elastin peptides on UVB-induced epidermal thickness, dorsal skin sections of hairless mice were stained with HE (Figure 3). Compared with the Control group (Figure 3A), epidermal thickness was markedly increased in the UV group mice. In addition, thickening of the stratum corneum and compact orthokeratosis were observed, as was remarkable vacuolar degeneration in the granular layer, prickle-cell layer, and basal layer, just below the stratum corneum (Figure 3B,E). In the PL mice, epidermal thickening was localized and discontinuously distributed, and vacuolar degeneration was rare and very mild or barely noticeable (Figure 3C,E). In addition, hyperkeratosis, compact orthokeratosis, and parakeratosis were observed in some cases. In the EL mice, the epidermis showed a nearly uniform thickness. Although the thickening of the stratum corneum was suppressed, compact orthokeratosis was observed (Figure 3D,E).

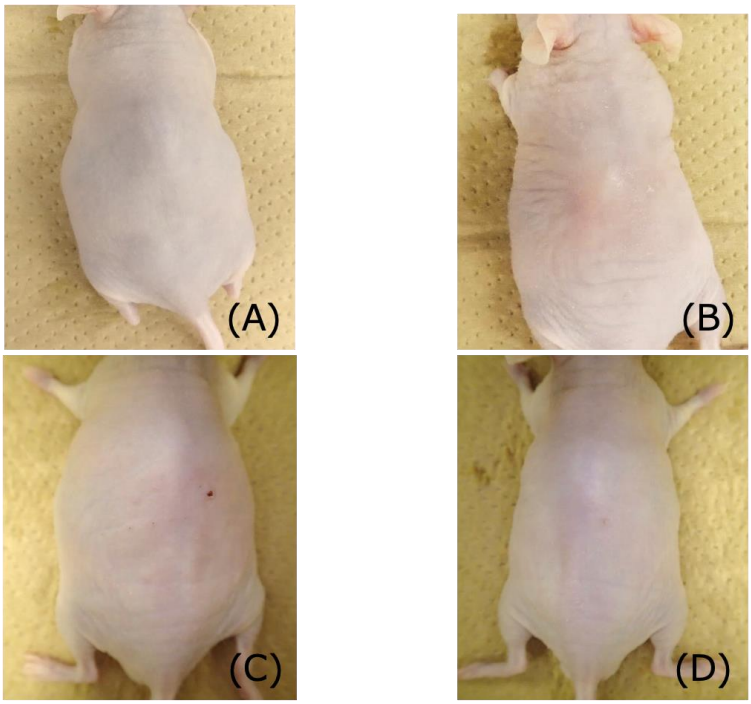

Figure 2. Macroscopic findings on the dorsal skin of hairless mice. (**A**) Control: dorsal skin of mice without UVB exposure; (**B**) UV: dorsal skin of mice that were not treated after UVB exposure; (**C**) PL: dorsal skin of mice to which placebo lotion was applied after UVB exposure; (**D**) EL: dorsal skin of mice to which 1% β-elastin lotion was applied after UVB exposure.

3.6. mRNA Expression of Ki67, p53, and Growth Factors in Skin Samples

To clarify the relationship between UVB exposure and cell growth, we also examined *Ki67* expression. As shown in Figure 3F, the expression of *Ki67* mRNA was upregulated in the UV and PL groups compared with the Control group. However, it was suppressed in the EL group compared with the Control group. We also examined whether EL inhibited the expression of *p53* and cell growth factors at the mRNA level in UVB-irradiated hairless mice. The *p53* and *TGF* mRNAs were significantly downregulated in the UV group (*p53*: 30.5% of the Control group, Dunnett's test $p < 0.01$, *TGF*: 36% of the Control group, Dunnett's test $p < 0.01$) compared with the Control group. However, no effect was found after the treatment with PL and EL. *EGF* expression levels in the three UVB-treated groups were significantly lower than in the Control group (UV: 28%, PL: 28%, EL: 24% that of the Control group, Dunnett's test $p < 0.01$).

3.7. Collagen and Elastin Contents in Dermal Tissue

The outward manifestations of photoaging primarily involve the two major structural proteins of the body, collagen and elastin [3]. To elucidate the effect of UVB irradiation on dermal collagen and elastin in photoaging development, we performed EVG staining to measure the ratios of each protein. The collagen ratios were higher, and the elastin ratios were lower in the dermis after 18 weeks of UVB irradiation (UV, PL, EL groups) compared with in the Control group, but the difference was not significant (Table 2). There was, however, an increase in the elastic fiber area fraction percentage throughout the dermis of the EL mice compared with the UV and PL mice, although the difference was not statistically significant at the 95% confidence level. Because the UVB irradiation conditions in this study were mild [22], the collagen/elastin ratios determined by EVG staining showed no effect of UVB or EL application.

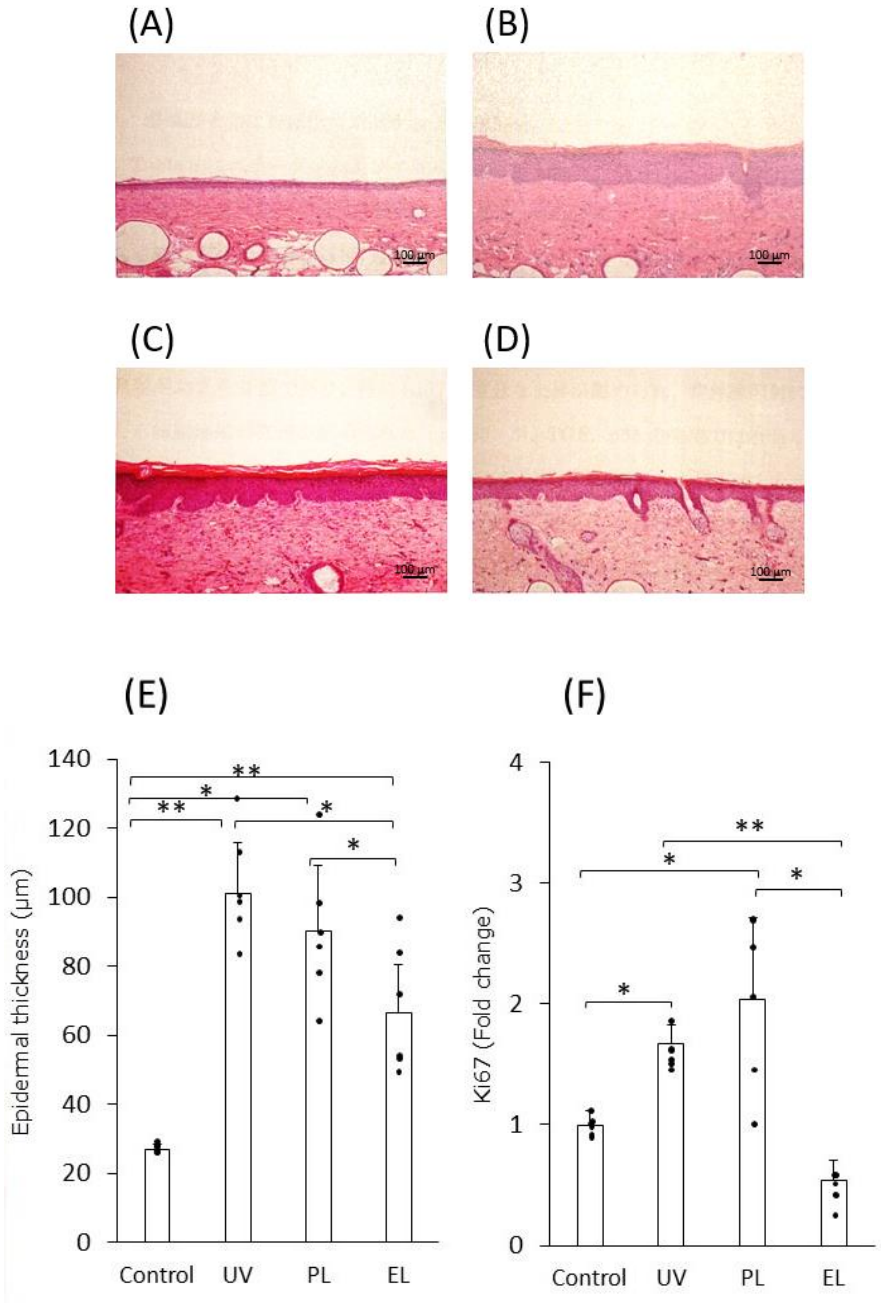

Figure 3. Comparison of epidermal thickness and expression of *Ki67*. (**A**–**D**) HE staining of the section of skin. (**A**) Control; (**B**) UV; (**C**) PL; (**D**) EL; (**E**) comparison of epidermal thickness; (**F**) comparison of *Ki67* mRNA expression. Mean ± S.D., Tukey's honestly significant difference test, * $p < 0.05$, ** $p < 0.01$. $n = 6$ in each group.

Table 2. Collagen and elastin contents of dermal tissues after 18 weeks of UVB irradiation.

Group	Collagen	Elastin
Control	65.050 ± 0.018	0.738 ± 0.246
UV	66.884 ± 0.011	0.349 ± 0.116
PL	67.263 ± 0.001	0.323 ± 0.234
EL	67.383 ± 0.017	0.498 ± 0.244

Mean ± S.D., Tukey's honestly significant difference test, n.s. n = 6 in each group.

3.8. Effects of EL on Glo1, DPP-IV, and MMP Expression in Skin Samples

Furthermore, to clarify the anti-inflammatory effects of EL, we compared *glyoxalase 1* (*Glo1*, key enzyme of glucose metabolism), *DPP-IV*, and *MMP-12* expression in skin samples. The expression of *Glo1* was upregulated in the UV and PL groups compared with the Control group ($p < 0.01$). This upregulation was suppressed in the EL group, which showed the same expression level as the non-UVB-irradiated Control group (Figure 4A). *DPP-IV* and *MMP-12* mRNA levels were upregulated in the UV group compared with the Control group but were downregulated in the lotion-treated groups [*DPP-IV*: UV vs. PL $p < 0.05$, UV vs. EL: $p < 0.01$ (Figure 4B), *MMP-12*: UV vs. PL or EL, $p < 0.05$ (Figure 4C)]. However, no significant difference in *MMP-1* mRNA expression was found.

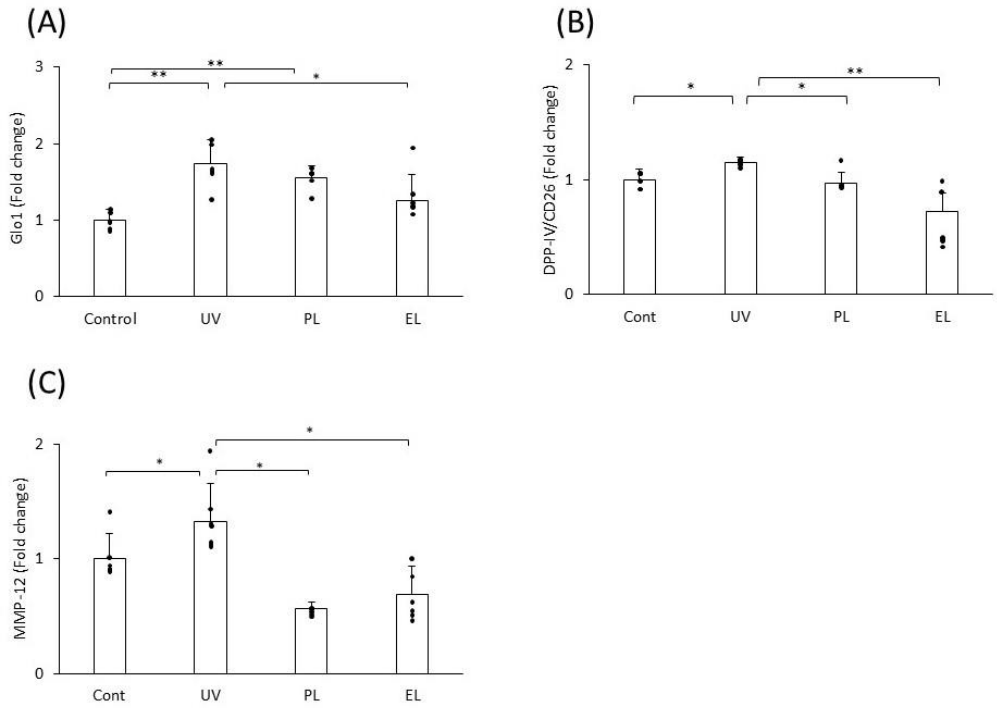

Figure 4. Effects of EL on *Glo1*, *DPP-IV*, and *MMP-12* expression of the section of skin. (**A**) *Gol1*; (**B**) *DPP-IV*; (**C**) *MMP-12*. Mean ± S.D., Tukey's honestly significant difference test, * $p < 0.05$, ** $p < 0.01$. n = 6 in each group.

4. Discussion

Skin aging is accelerated by a combination of external factors, such as UV radiation, nutritional conditions, oxidative stress, DNA damage, and various other stresses [1–7]. Photoaging is the most important factor causing skin damage and aging. Various food components have been investigated for potential protective effects on the skin [4]. The significant antioxidant and anti-inflammatory activities of some components have been reported, followed by the ability to modulate immune functions in the skin. Our previous studies showed that the oral administration of elastin hydrolysates protected against vascular injuries [16].

In this study, we evaluated the effects and efficiency of topically applied peptides from the protein hydrolysates of bulbus arteriosus elastin in a UVB-induced photodamaged mouse model, and clarified that the peptides improved the epidermal conditions. To the best of our knowledge, this is the first demonstration that EL with DPP-IV/CD26 inhibition contributes to the suppression of photoaging.

In this study, we demonstrated that topical treatment with EL, which shows DPP-IV/CD26 inhibitory activity, significantly attenuated the increase in epidermal thickness induced by chronic UVB irradiation. Senescent cells are characterized by the secretion of fac-

tors that promote inflammation and tissue deterioration [23]. These senescence-associated changes in skin cells are significant in wound healing, fibrotic disorders, and skin cancer, in which DPP-IV/CD26 inhibition downregulates the effects of pro-fibrotic proteins and cytokines, ultimately improving cutaneous diseases [11]. EL reduced epidermal thickness, accompanied by the suppression of Ki67 expression. Although cellular senescence was originally defined as an irreversible form of cell cycle arrest, the emergence of proliferative cells that have escaped senescence has been reported by several groups [9,24]. Tóth et al. showed that the expression of both Ki67 and a new senescence marker, DPP-IV/CD26, was significantly increased in senescent MCF-7 breast cancer cells, and the combination of a senolytic drug (azithromycin) and a DPP-IV/CD26 inhibitor (sitagliptin) exerted a synergistic effect in senescent MCF-7 cells, reducing the number of cells escaping senescence [9]. Although no changes in *p53* or growth factor expression were observed in this study, the expression of *Ki67* and *DPP-IV* changed under the influence of UVB irradiation and EL application. Therefore, these results indicate that EL attenuates epidermal thickening associated with cell growth, mediated by DPP-IV/CD26 inhibition. Furthermore, measurement of epidermal DPP-IV/CD26 expression may help to prevent the skin inflammation that leads to precancerous conditions, as well as aid in the diagnosis of skin inflammation and treatment for the removal of cells that have escaped senescence.

The denaturation and fragmentation of collagen and elastin fibers may lead to skin wrinkling and sagging, which are important symptoms of skin photoaging [25]. In this study, the topical application of EL to the skin inhibited the expression of Glo1 induced by UVB irradiation. In the glycolysis system, a trace of the highly reactive α-dicarbonyl compound methylglyoxal is constantly produced as a by-product by glyceraldehyde-3-phosphate, an intermediate product of glucose metabolism. Methylglyoxal exhibits strong cytotoxicity. Normally, methylglyoxal is eliminated by the glyoxalase system, in which the key enzyme is Glo1. In a diabetic state, the downregulation of Glo1 and the upregulation of methylglyoxal increase the accumulation of AGEs in the body, which is thought to exacerbate diabetic complications.

Conversely, in the diagnosis of cancers, in which a large amount of glucose is taken in and the glycolysis system is activated, Glo1 is observed to be highly expressed [26]. It has also been reported that Glo1 is upregulated in aged skin [27]. Therefore, our data indicated that EL ameliorated the excess activation of glucose metabolism and cell senescence by UVB irradiation. It is well established that the degradation of collagen and elastin fiber networks in the skin is promoted by MMPs [3]. In particular, MMP-1 and MMP-12 may degrade the main structural proteins of the skin (type I and III collagen) and elastin, thereby causing wrinkles and sagging in photodamaged skin [28]. In this study, the expression of *MMP-12* was increased by UVB irradiation, but this abnormal process was suppressed by lotion treatment. However, no changes in the expression of *MMP-1* in the skin samples or the ratio of collagen fibers and elastin in the dermis were observed. Further investigations are needed to clarify the mechanism of the observed qualitative changes, including modifications and crosslinking of collagen and elastin due to photoaging, and the function of EL in preventing such changes.

As a result, in this study, no damage to the skin due to the decomposition of collagen and elastin caused by activation of MMPs was observed. This is thought to be because the UVB irradiation used in this study was at a relatively low energy intensity [22], so there was little damage to the skin. However, improvement of epidermal thickness due to EL via the Ki67 gene expression was observed. Furthermore, it was thought that the anti-inflammatory activity (DPP-IV/CD26) of EL suppressed the senescence of epidermal cells and was involved in the skin condition.

Age-related morphological changes include wrinkling and sagging of the skin on the face. The effects of photoaging caused by UV (UVA and UVB) have been reported as the main factor in aggravating these changes, and this photoaging is distinct from natural aging that occurs in non-UV-exposed areas. Among the parts of the human face, the formation of wrinkles is observed earliest at the corners of the eyes, and, with age, the frequency of

exposure to UV increases, and, in areas where skin elasticity decreases, quantitative and qualitative changes occur in collagen and elastin [3]. In this study, although the formation of wrinkles under continuous mild UVB irradiation was confirmed, it was not accompanied by changes in the composition of collagen and elastin in the dermis. It is speculated that there are some limitations in accurately reflecting the condition of human skin in present studies using UV irradiation on hairless mice. Although clinical trials can be employed to morphologically verify the effects of nutritional ingredients on the skin [29], animal models and culture cells are required for elucidating the mechanisms involved. In the current study, the effects of EL were mediated through the prevention of epidermal thickening and the improvement of the expression of various enzymes due to UVB irradiation.

In conclusion, although there have been previous reports of DPP-IV/CD26 inhibition in wound healing, we are the first to demonstrate that EL, which shows DPP-IV/CD26 inhibition activity, can contribute to the suppression of photoaging, a possible cause of skin cancer, through the inhibition of cellular senescence. Previous research into photoaging has focused on structural changes in skin collagen and elastin and the activation of their degradative enzymes, the increased production of ROS and inflammatory cytokines [30], and the MARK signaling pathway, including P38 and JNK [31]. Future research into photoaging will need to examine the involvement of DPP-IV/CD26 in improving cellular aging.

Author Contributions: T.K., E.Y., E.S. and T.C. performed the experiments and analyzed the data. T.K. and K.T. wrote the manuscript. T.K. and K.T. conceptualized the study and coordinated project administration. All authors have read and agreed to the published version of the manuscript.

Funding: This research was funded by a Grant-in-Aid for Scientific Research (C) (General), 22K11791.

Institutional Review Board Statement: Institutional Review Board Statement: "The animal study protocol was approved by Kindai University Animal Experiment Committee (KAAG-25-010)".

Informed Consent Statement: Not applicable.

Data Availability Statement: The raw data supporting the conclusions of this article will be made available by the authors on request.

Acknowledgments: We would like to acknowledge our appreciation for the technical support of Katsumi Okumoto (Life Science Research Institute, Kindai University) and Tomoko Hashimoto (Centre for Morphological Analyses, Central Research Facilities, Kindai University Faculty of Medicine).

Conflicts of Interest: Author Eri Shiratsuchi was employed by the company R & D Division, Hayashikane Sangyo Co., Ltd., and author Takashi Kometani was employed by the company Pharma Foods International, Co., Ltd. The remaining authors declare that the research was conducted in the absence of any commercial or financial relationships that could be construed as a potential conflict of interest.

References

1. D'Orazio, J.; Jarrett, S.; Amaro-Ortiz, A.; Scott, T. UV radiation and the skin. *Int. J. Mol. Sci.* **2013**, *14*, 12222–12248. [CrossRef] [PubMed]
2. Bernstein, E.F.; Chen, Y.Q.; Kopp, J.B.; Fisher, L.; Brown, D.B.; Hahn, P.J.; Robey, F.A.; Lakkakorpi, J.; Uitto, J. Long-term sun exposure alters the collagen of the papillary dermis. *J. Am. Acad. Dermatol.* **1996**, *34*, 209–218. [CrossRef] [PubMed]
3. Lee, H.; Hong, Y.; Kim, M. Structural and functional changes and possible molecular mechanisms in aged skin. *Int. J. Mol. Sci.* **2021**, *22*, 12489. [CrossRef] [PubMed]
4. Fernandes, A.; Rodrigues, P.M.; Pintado, M.; Tavaria, F.K. A systematic review of natural products for skin applications: Targeting inflammation, wound healing, and photo-aging. *Phytomedicine* **2023**, *115*, 154824. [CrossRef]
5. Gkogkolou, P.; Böhm, M. Advanced glycation end products: Key players in skin aging? *Dermato-Endocrinology* **2012**, *4*, 259–270. [CrossRef]
6. Mizutari, K.; Ono, T.; Ikeda, K.; Kayashima, K.; Horiuchi, S. Photo-enhanced modification of human skin elastin in actinic elastosis by N(epsilon)-(carboxymethyl)lysine, one of the glycoxidation products of the Maillard reaction. *J. Investig. Dermatol.* **1997**, *108*, 797–802. [CrossRef]
7. Pittayapruek, P.; Meephansan, J.; Prapapan, O.; Komine, M.; Ohtsuki, M. Role of matrix metalloproteinases in photoaging and photocarcinogenesis. *Int. J. Mol. Sci.* **2016**, *17*, 868. [CrossRef]

8. Singh, A.K. Dipeptidyl peptidase-4 inhibitors: Novel mechanism of actions. *Indian. J. Endocrinol. Metab.* **2014**, *18*, 753–759. [CrossRef]
9. Tóth, F.; Moftakhar, Z.; Sotgia, F.; Lisanti, M.P. In Vitro investigation of therapy-induced senescence and senescence escape in breast cancer cells using novel flow cytometry-based methods. *Cells* **2024**, *13*, 841. [CrossRef]
10. Kim, K.M.; Noh, J.H.; Bodogai, M.; Martindale, J.L.; Yang, X.; Indig, F.E.; Basu, S.K.; Ohnuma, K.; Morimoto, C.; Johnson, P.F.; et al. Identification of senescent cell surface targetable protein DPP4. *Genes Dev.* **2017**, *31*, 1529–1534. [CrossRef]
11. Patel, P.M.; Jones, V.A.; Kridin, K.; Amber, K.T. The role of dipeptidyl peptidase-4 in cutaneous disease. *Exp. Dermatol.* **2021**, *30*, 304–318. [CrossRef] [PubMed]
12. Jones, L.; Jones, A.M. Suspected adverse drug reactions of the type 2 antidiabetic drug class dipeptidyl-peptidase IV inhibitors (DPP4i): Can polypharmacology help explain? *Pharmacol. Res. Perspect.* **2022**, *10*, e01029. [CrossRef] [PubMed]
13. Majid, A.; Lakshmikanth, M.; Lokanath, N.K.; Poornima Priyadarshini, C.G. Generation, characterization and molecular binding mechanism of novel dipeptidyl peptidase-4 inhibitory peptides from sorghum bicolor seed protein. *Food Chem.* **2022**, *369*, 130888. [CrossRef] [PubMed]
14. Zhang, M.; Zhu, L.; Wu, G.; Liu, T.; Qi, X.; Zhang, H. Rapid screening of novel dipeptidyl peptidase-4 inhibitory peptides from pea (*Pisum sativum* L.) protein using peptidomics and molecular docking. *J. Agric. Food Chem.* **2022**, *70*, 10221–10228. [CrossRef] [PubMed]
15. Heinz, A. Elastic fibers during aging and disease. *Ageing Res. Rev.* **2021**, *66*, 101255. [CrossRef]
16. Takemori, K.; Yamamoto, E.; Ito, H.; Kometani, T. Prophylactic effects of elastin peptide derived from the bulbus arteriosus of fish on vascular dysfunction in spontaneously hypertensive rats. *Life Sci.* **2015**, *120*, 48–53. [CrossRef]
17. Halabi, C.M.; Mecham, R.P. Elastin purification and solubilization. *Methods Cell Biol.* **2018**, *143*, 207–222.
18. Lansing, A.I.; Rosenthal, T.B.; Alex, M.; Dempsey, E.W. The structure and chemical characterization of elastic fibers as revealed by elastase and by electron microscopy. *Anat. Rec.* **1952**, *114*, 555–575. [CrossRef]
19. Partridge, S.M.; Davis, H.F. The chemistry of connective tissues. 3. Composition of the soluble proteins derived from elastin. *Biochem. J.* **1955**, *61*, 21–30. [CrossRef]
20. Partridge, S.M.; Davis, H.F.; Adair, G.S. The chemistry of connective tissues. 2. Soluble proteins derived from partial hydrolysis of elastin. *Biochem. J.* **1955**, *61*, 11–21. [CrossRef]
21. Nakaba, M.; Ogawa, K.; Seiki, M.; Kunimoto, M. Properties of soluble elastin peptide from bulbus arteriosus in fish species. *Fish. Sci.* **2006**, *72*, 1322–1324. [CrossRef]
22. Kawada, S.; Ohtani, M.; Ishii, N. Increased oxygen tension attenuates acute ultraviolet-B-induced skin angiogenesis and wrinkle formation. *Am. J. Physiol. Regul. Integr. Comp. Physiol.* **2010**, *299*, 694–701. [CrossRef] [PubMed]
23. Walen, K.H. Genetic stability of senescence reverted cells: Genome reduction division of polyploidy cells, aneuploidy and neoplasia. *Cell Cycle* **2008**, *7*, 1623–1629. [CrossRef] [PubMed]
24. Höhn, A.; Weber, D.; Jung, T.; Ott, C.; Hugo, M.; Kochlik, B.; Kehm, R.; König, J.; Grune, T.; Castro, J.P. Happily (n)ever after: Aging in the context of oxidative stress, proteostasis loss and cellular senescence. *Redox Biol.* **2017**, *11*, 482–501. [CrossRef]
25. Wondrak, G.T.; Jacobson, E.L.; Jacobson, M.K. Photosensitization of DNA damage by glycated proteins. *Photochem. Photobiol. Sci.* **2002**, *1*, 355–363. [CrossRef]
26. Sakamoto, H.; Mashima, T.; Sato, S.; Hashimoto, Y.; Yamori, T.; Tsuruo, T. Selective activation of apoptosis program by S-p-bromobenzylglutathione cyclopentyl diester in glyoxalase I-overexpressing human lung cancer cells. *Clin. Cancer Res.* **2001**, *7*, 2513–2518.
27. Yumnam, S.; Subedi, L.; Kim, S.Y. Glyoxalase system in the progression of skin aging and skin malignancies. *Int. J. Mol. Sci.* **2020**, *22*, 310. [CrossRef]
28. Wang, D.; Zhou, Y.; Zhao, J.; Ren, C.; Yan, W. Oral yak whey protein can alleviate UV-induced skin photoaging and modulate gut microbiota composition. *Foods* **2024**, *13*, 2621. [CrossRef]
29. Wyles, S.P.; Proffer, S.L.; Farris, P.; Randall, L.; Hillestad, M.L.; Lupo, M.P.; Behfar, A. Effect of topical human platelet extract (HPE) for facial skin rejuvenation: A histological study of collagen and elastin. *J. Drugs Dermatol.* **2024**, *23*, 735–740. [CrossRef]
30. Xiang, X.W.; Zheng, H.Z.; Wang, R.; Chen, H.; Xiao, J.X.; Zheng, B.; Liu, S.L.; Ding, Y.T. Ameliorative Effects of Peptides Derived from Oyster (*Crassostrea gigas*) on Immunomodulatory Function and Gut Microbiota Structure in Cyclophosphamide-Treated Mice. *Mar. Drugs* **2021**, *19*, 456. [CrossRef]
31. Gu, M.J.; Lee, H.W.; Yoo, G.; Kim, D.; Choi, I.W.; Kim, Y.; Ha, S.K. Protective effect of Schizonepeta tenuifolia Briq. ethanolic extract against UVB-induced skin aging and photodamage in hairless mice. *Front. Pharmacol.* **2023**, *14*, 1176073. [CrossRef]